Photobioelectrocatalysis of Intact Photosynthetic Bacteria Exposed to Dinitrophenol

Lilian Danielle de Moura Torquato,[a, b, c] Rosa Maria Matteucci,[a] Paolo Stufano,[d] Danilo Vona,[a] Gianluca M. Farinola,[a] Massimo Trotta,[e] Maria Valnice Boldrin Zanoni,[b, c] and Matteo Grattieri*[a, e]

The outstanding metabolic versatility of purple non-sulphur bacteria makes these organisms an ideal candidate for developing photobioelectrochemical systems applicable in contaminated environments. Here, the effects of 2,4 dinitrophenol, a common contaminant, on purple bacteria photobioelectrocatalysis were investigated. The aromatic contaminant clearly affects current generation, with an enhanced photocurrent obtained at low dinitrophenol concentrations (0.5–1 µM), while higher values (up to 100 µM) resulted in a gradual decrease of photocurrent. The obtained electrochemical evidence, coupled to spectroscopic studies, allowed verifying the viability of the bacteria cells after exposure to dinitrophenol, and that no alteration of the photosynthetic apparatus was obtained. The results indicate that high dinitrophenol concentrations divert electrons from the extracellular electron pathway to an alternative electron sink. The present results open the door to the possible use of intact bacteria-based photoelectrodes to develop technologies for sustainable biosensors with simultaneous environmental remediation.

Introduction

During billions of years of evolution, nature has found different ways to utilize sunlight as energy source by means of complex and sophisticated photosystems, which evolved from the photosynthetic unit of purple bacteria. *Rhodobacter capsulatus* (*R. capsulatus*) is a purple non-sulfur photosynthetic bacterium (PNSB) that exhibits an outstanding metabolic versatility, allowing this organism to grow under diverse environmental conditions.[1] Photoheterotrophic growth is typical for PNSB, which can use a range of organic compounds such as organic acids, amino acids, fatty acids, alcohols, carbohydrates, and aromatic compounds as electron and carbon sources. Under phototrophic growth conditions, organic carbon sources serve primarily as cellular carbon for PNSB, but may also function as electron source for photosynthetic electron transport.[2] Hence, during photosynthesis, organic compounds play the role of electron donors. The obtained electrons are energized by the photosystem upon light excitation (pathway 1 in Scheme 1), feeding a cyclic flow of electrons and protons. This process results in a proton-motive force driving ATP synthesis, while electrons are utilized for $NADP^+$ reduction, generating NADPH (pathway 3 in Scheme 1), or can be repeatedly excited and cycled[3] (pathway 2 in Scheme 1).

The photosynthetic system of purple bacteria has been characterized in details,[4,5] unveiling the process of sunlight conversion into electrical energy with efficiency approaching unity.[6] With the aim to take advantage of this unique catalytic features, these bacteria have been recently coupled to electrode surfaces for the transduction of solar energy into electrical energy, hydrogen, or high added-value chemicals in photobioelectrochemical systems (PBES).[7] To enable the photo-induced extracellular electron transfer (PEET) process using intact PNSB in these devices, a coherent interface between the electrode surface and the redox active sites of the photosynthetic apparatus that are deeply buried in the inner membrane (i.e., quinone pool) must be obtained.[8–10] The electrical wiring can be achieved by using exogeneous redox mediators, with several diffusible quinone-based redox mediators that can shuttle the electrons during PEET process.[11] However, the application of diffusible mediators in the field is not preferable owing to their toxicity and unwanted release

[a] Dr. L. D. de Moura Torquato, R. M. Matteucci, Dr. D. Vona, Prof. G. M. Farinola, Dr. M. Grattieri
Department of Chemistry
Università degli Studi di Bari "Aldo Moro"
via E. Orabona 4, Bari, 70125 (Italy)
E-mail: matteo.grattieri@uniba.it

[b] Dr. L. D. de Moura Torquato, Prof. M. V. Boldrin Zanoni
Institute of Chemistry
São Paulo State University (UNESP)
Rua Prof. Francisco Degni, 55, Araraquara, SP, 14800-060 (Brazil)

[c] Dr. L. D. de Moura Torquato, Prof. M. V. Boldrin Zanoni
National Institute for Alternative Technologies of Detection
Toxicological Evaluation and Removal of Micropollutants and Radioactives (INCT-DATREM)
São Paulo State University (UNESP)
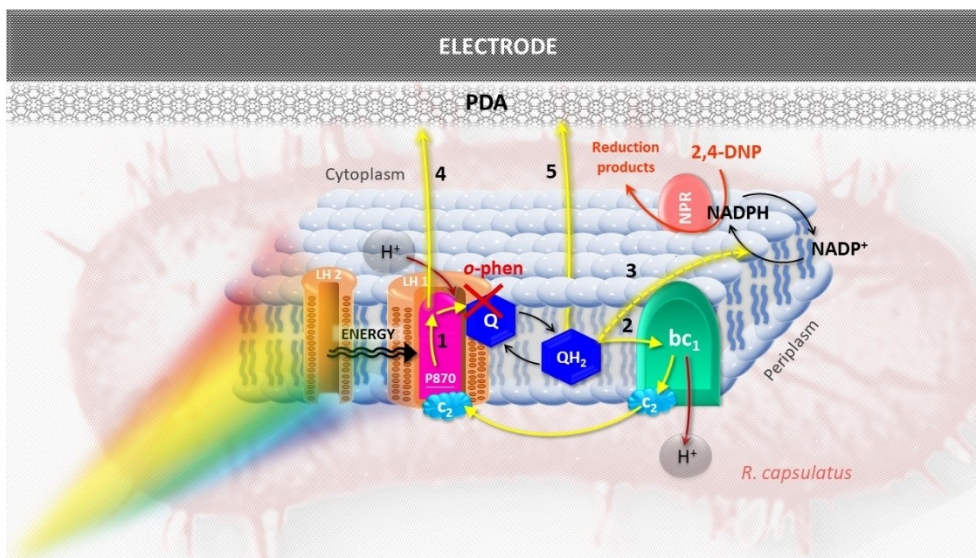Rua Prof. Francisco Degni, 55, Araraquara, SP, 14800-060 (Brazil)

[d] Dr. P. Stufano
CNR-NANOTEC, Institute of Nanotechnology
Consiglio Nazionale delle Ricerche
via E. Orabona 4, Bari, 70125 (Italy)

[e] Dr. M. Trotta, Dr. M. Grattieri
IPCF-CNR Istituto per i Processi Chimico Fisici
Consiglio Nazionale delle Ricerche
via E. Orabona 4, Bari, 70125 (Italy)

Scheme 1. Representation of the photosynthetic electron cycle and electron sinks of *R. capsulatus* under photobioelectrocatalytic conditions in presence of 2,4-DNP. The electrons flow, the protons flow, and the reduction of 2,4-DNP are represented in yellow, red, and orange, respectively.

into the environment.[10,11] As a result, various studies have focused on the use of alternatives to diffusible mediators.[12,13] Recent reports showed the engineering of photosynthetic bacteria by genetic strategies,[14] and with carbon nanotubes,[15] which facilitated the extracellular electron transfer process. Another possibility involves the use of redox polymers, where the redox moieties are confined on the polymer backbone. Such works include the use of both Os-based,[16] and quinone-based polymers.[17] Our group recently reported the possibility to obtain a redox-adhesive matrix based on polydopamine (PDA) to obtain purple bacteria-based photoelectrodes without the need of a separate synthesis of the redox polymer.[18] The obtained PBES can be employed for a broad range of applications. Specifically, with the increasing interest in systems for the early monitoring of environmental hazards,[19] the development of biosensors for distributed analysis is of the utmost importance. In these systems, the generated current can be directly related to the presence of contaminants, allowing their preliminary on-line monitoring,[20] and enabling self-powered biosensors.[21–23] In addition, thanks to the capability of PNSB to degrade organic compounds that are environmental pollutants, these PBES can be employed for sun-powered decontamination and monitoring of water environments.[24] In this work, 2,4-dinitrophenol (2,4-DNP) was utilized as a model contaminant to study its effects on the PDA-based biophotoelectrode. 2,4-DNP is a commercially relevant dinitrophenol commonly found in several industrial wastewater due to its use in the manufacture of dyes, wood preservatives, explosives, and as a pesticide.[25] Due to its frequent occurrence, high toxicity, and recalcitrance in environment, 2,4-DNP is considered as one of the priority pollutants by the US Environmental Protection Agency.[26] The acute and chronic toxic concentrations of 2,4-DNP for freshwater aquatic species (5th percentile) were reported to be up to 14.4 and 2.3 μM, respectively.[27] Classical analytical techniques, such as high-performance liquid chroma-

tography allow the detection of 2,4-DNP down to 1 μM.[28] Alternative approaches have been proposed for nitrophenol monitoring,[29] including voltammetric studies showing its detection in concentrations as low as 0.7 μM.[30] However, the reported approach required acid conditions and 80% methanol, and detected the metabolite of 2,4-dinitrophenol (i.e., 2-amino-4-nitrophenol and 4-amino-2-nitrophenol). In a recent study, a multistage microbial fuel cell inoculated with wastewater was utilized as a biosensor for 4-nitrophenol monitoring as model contaminant, and possible removal.[31] It was shown that the contaminant influenced current production of the microbial fuel cell for concentrations higher than 540 μM (75 mg L^{-1}), while lower concentrations did not affect the performance of the device. This work targets the development of a biophotoelectrode where the concentrations of dinitrophenol affecting photobioelectrocatalysis match the values reported for acute and chronic toxicity of this contaminant, with the future goal to develop an early-monitoring and bioremediation system powered by sunlight.

Results and Discussion

Effect of 2,4-DNP on photobioelectrocatalysis

Photobioelectrocatalysis of the biohybrid electrode obtained by entrapping *R. capsulatus* in PDA (*R.caps*-PDA) was studied by cyclic voltammetry. Figure 1 shows the current response for the biophotoelectrode and control electrodes under anaerobic conditions (no bacteria, only PDA modified electrodes) in dark and exposed to light, in the presence or absence of 2,4-DNP. Specifically, Figure 1A shows the dark metabolism of *R. capsulatus* in the presence of malic acid (trace 2), and malic acid with ethanol (trace 3), given the increased current obtained for the *R.caps*-PDA electrodes in relation to the sterile electrode
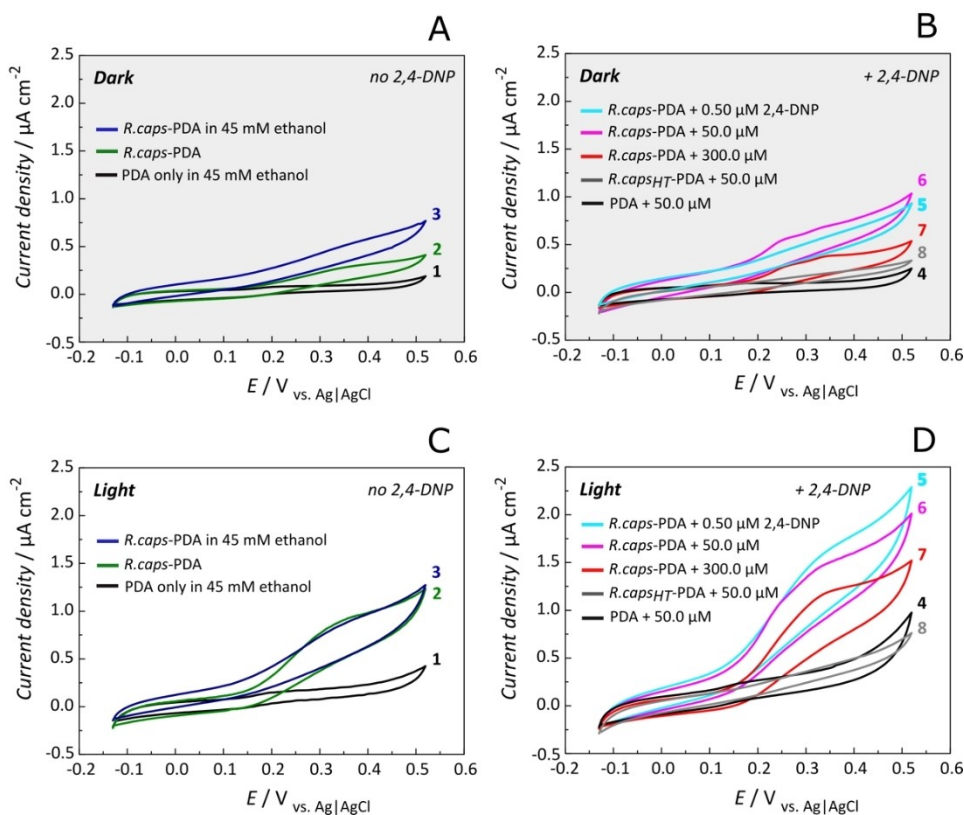
Figure 1. Cyclic voltammetries for *R.caps*-PDA biohybrid photoanodes and PDA control electrodes in the absence (A and C) or presence (B and D) of 2,4-DNP. The gray background indicates CVs performed under dark conditions, while the white background indicates the experiments performed under light conditions. (1) PDA-only in 50 mM malic acid. (2) *R.caps*-PDA in 50 mM malic acid. (3) *R.caps*-PDA in 50 mM malic acid + 45 mM ethanol. All the other traces refer to experiments performed with 50 mM malic acid + 45 mM ethanol with various concentrations of DNP as following defined: (4) PDA + 50.0 μM 2,4-DNP; (5) *R.caps*-PDA + 0.50 μM 2,4-DNP; (6) *R.caps*-PDA + 50.0 μM 2,4-DNP; (7) *R.caps*-PDA + 300.0 μM 2,4-DNP; (8) *R.caps*$_{HT}$-PDA + 50.0 μM 2,4-DNP. Scan rate:1 mV s^{-1}; CE: Pt; RE: Ag|AgCl (3 M NaCl).

coated with only PDA (trace 1). Following, the biocatalytic activity of the biohybrid system was evaluated under increasing additions of 2,4-DNP (Figure 1B). The assimilation of 2,4-DNP in the range of 0.5 to 50.0 μM (traces 5 and 6) promoted the generation of higher dark currents. On the other hand, raising the concentration of 2,4-DNP to 300.0 μM (trace 7) resulted in a decrease of current to values close to those obtained prior DNP addition. It should be noted that the current of the sterile control electrode (trace 4) did not change even when the DNP concentration was raised to 50 μM. Furthermore, a negligible current was observed for the biohybrid electrode prepared utilizing heat treated *R. capsulatus* cells (*R.caps*$_{HT}$-PDA, trace 8) at 50 μM 2,4-DNP, confirming that viable *R. capsulatus* cells are required to obtain a catalytic current, and the existence of a dark metabolism for the assimilation of 2,4-DNP under the utilized experimental conditions. Figure 1C shows the photo-bioeletrocatalytic activity (experiments under illumination) of *R.caps*-PDA electrodes in relation to the sterile electrode. PDA control electrodes presented a slight increase in current as expected considering the broadband UV-vis absorption ability of PDA.[32] On the other hand, biohybrid electrodes achieved up to 2-fold enhancement in current density in relation to that observed for the dark metabolism in the presence of only malic acid, passing from 0.44 ± 0.05 to 1.02 ± 0.28 μA cm^{-2} (trace 2).
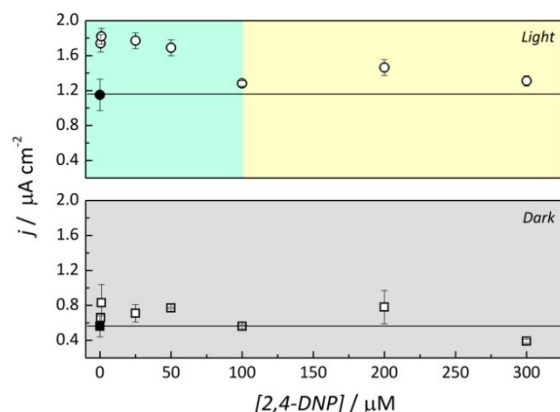
When adding 0.5 μM 2,4-DNP (Figure 1D), the biophotoanode showed a remarkable increment in current density achieving up to 2.2 ± 0.1 μA cm^{-2} (trace 5). Further increasing the concentration of 2,4-DNP up to 300 μM (trace 7) resulted in a gradual decrease in current density to 1.57 ± 0.07 μA cm^{-2}. The sterile electrode (trace 4) showed a slight increase in current density in presence of 50 μM 2,4-DNP, possibly due to its reaction with the PDA matrix. When the same concentration of 2,4-DNP was evaluated with the biotic control electrode *R.caps*$_{HT}$-PDA (trace 8), no significant change in current density was observed in relation to the dark experiment performed under the same conditions, which further confirmed the photobioelectrocatalytic activity for assimilation of this aromatic compound by *R. capsulatus*. Additionally, for the cyclic voltammetries performed with the biophotoelectrodes in the absence of 2,4-DP, both in dark and light conditions, a clear single redox peak at about + 0.31 V vs. Ag|AgCl can be noted. This characteristic redox feature is due to the extracellular electron transfer process mediated by the PDA matrix, as reported in our previous work.[18] Conversely, the cyclic voltammetries of the biophotoelectrodes in the presence of 2,4-DNP showed two redox peaks at about + 0.22 and + 0.31 V vs. Ag|AgCl, respectively. This characteristic response was not obtained for the sterile electrodes nor for the electrode with heat-treated cells exposed to 2,4-

ChemElectroChem

Research Article
doi.org/10.1002/celc.202300013

Chemistry
Europe
European Chemical
Societies Publishing

DNP. Accordingly, the appearance of the additional redox peaks at $+0.22$ V in presence of 2,4-DNP indicates that under such conditions the extracellular electron transfer process can take place utilizing an additional electron transfer pathway, such as diffusible reduced endogenous mediators (i.e., quinones) available in excess due to the contaminant acting as electron donor.

Previous works of Blasco and Castillo[33] reported that the uptake of 2,4-DNP by *R. capsulatus* is strictly light-dependent and inhibited in the presence of O_2 and ammonium, with an optimal pH of 7.0.[34] In their work the authors noted that none of the four nitrophenol tested could be assimilated by *R. capsulatus* under dark anaerobiosis. However, the metabolism of 2,4-DNP under bioelectrochemical conditions has never been investigated before the current study. The cyclic voltammetries presented in Figure 1 reveal that 2,4-DNP can be oxidized by *R. capsulatus* when the system is under electrochemical polarization. Focusing on the requirement of anaerobic conditions, cyclic voltammetries performed under aerobic conditions (Figure S1) showed no catalytic current when adding DNP, indicating no 2,4-DNP assimilation obtained under electrochemical polarization in presence of oxygen. These results confirmed the previous finding of Blasco and Castillo. The cyclic voltammetries of the biohybrid system in presence of oxygen showed only a marked current response due to the oxygen reduction reaction, with an onset of the cathodic current at -0.10 V, in either the absence or the presence of nitrophenol.
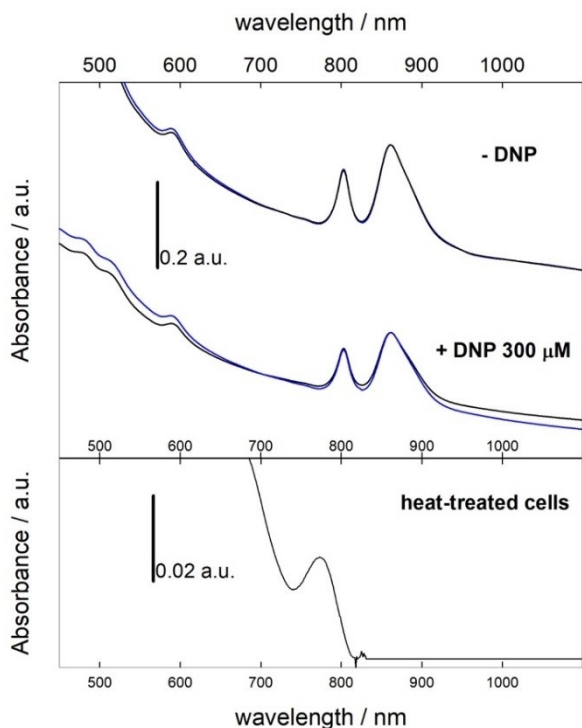
Based on the presented results, we investigated the effect of the different concentration of 2,4-DNP on the anaerobic photobioelectrocatalysis of *R. capsulatus*. Figure 2 shows the average values of current densities obtained at $+0.40$ V during the second anodic scan. The potential for the comparison was selected as under these conditions the photoanode *R.caps*-PDA reached a quasi-steady state current response for all the concentrations of 2,4-DNP evaluated. Under illumination, the biophotoanode presented different behaviors depending on

the concentration of 2,4-DNP (Figure 2, top). The addition of 0.5 and 1 μM 2,4-DNP led to the maximum current response obtained, reaching 1.82 ± 0.05 μA cm^{-2}, a value 50% higher than the photocurrent density produced in the absence of DNP. Further increasing the concentration of 2,4 DNP up to 100 μM resulted in a clear decrease in photocurrent, eventually reaching values comparable to the baseline current density achieve prior to the addition of the contaminant. An additional increase in 2,4-DNP concentration up to 300 μM resulted in current values ranging between 1.46 ± 0.09 and 1.31 ± 0.06 μA cm^{-2}, thus only slightly deviating from the values achieved at 100 μM 2,4-DNP. These results indicate that the application of the biophotoanode for 2,4-DNP monitoring would be limited to the concentration range 1–100 μM. However, it is interesting to note that this concentration range includes the limits for acute and chronic toxic concentrations reported for 2,4-DNP (14.4 and 2.3 μM, respectively), paving the way to future studies aimed to further develop a detection system based on the microbial biophotoanode reported. Another aspect deserving further discussion is that the current response for 2,4-DNP concentrations higher than 100 μM did not fall below the initial value obtained in absence of the contaminant, suggesting that a mechanism more complex than a simple cytotoxic effect is at play. This aspect is further discussed below, in view of spectroscopic and additional electrochemical experimental evidence. On the other hand, cyclic voltammetries in dark conditions with increasing concentration of 2,4-DNP revealed current densities close to the baseline values obtained in the absence of DNP, regardless the concentration of 2,4-DNP applied (Figure 2, bottom).

Spectroscopic studies were performed to investigate if the observed decreasing current response obtained for *R.caps*-PDA biophotoelectrodes exposed to DNP under illumination was due to damaging of the photosynthetic apparatus after exposure to the contaminant. Figure 3 (upper panel, upper traces) shows the UV-vis-NIR absorption spectrum of *R. capsulatus* entrapped in the PDA matrix in the absence of 2,4-DNP. The absorption band observed at 865 nm is associated to the light harvesting complex LH1 in intimate contact with the bacterial reaction center, in analogy to the observation on the bacterium *Rhodobacter sphaeroides* 2.4.1; the absorption band at 800 nm is associated to the light harvesting complex LH2 (see Scheme 1). The secondary bands of the LH complexes are at 590 nm.[35,36] The light-harvesting capacity of the bacteriochlorophylls pigments in the LHs complexes are complemented by the carotenoids, assigned to the bands in the spectral range between 420 and 510 nm. This broad spectral ability enables the efficient photoconversion ability of the reaction center.[37] As shown by the absorption spectrum of *R. capsulatus* entrapped in the PDA matrix in the presence of 300 μM 2,4-DNP (upper panel, lower traces), the exposure to the contaminant did not cause any damage to the antennae apparatus, neither immediately after addition (black trace), nor after 1 h (blue trace). The spectrum obtained from heat-treated bacteria used to prepare the *R.caps*-PDA electrode clearly show the disruption of the bacterial cells and denaturation of the LHs complexes, with the disappearing of the two peaks at 800 nm

Figure 2. Current densities obtained at $+0.40$ V for the *R.caps*-PDA photoanode exposed to 0.5, 1, 25, 50, 100, 200, and 300 μM 2,4-DNP under light (empty circles), and dark conditions (empty squares). The average values of current densities are reported with the respective standard deviations obtained from cyclic voltammetry studies performed in triplicate. Full symbols with a continuous line represent the current density obtained in each condition (light and dark) with *R.caps*-PDA electrode exposed only to 50 mM malic acid + 45 mM ethanol (baseline current density).
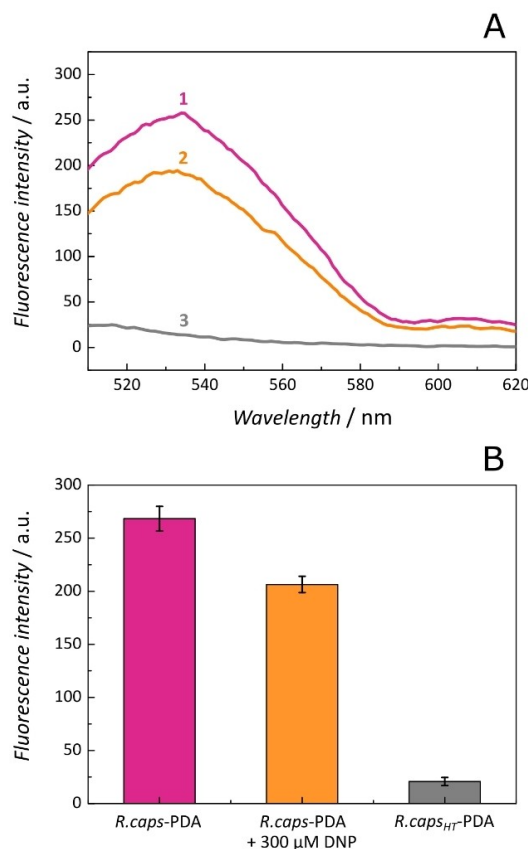
Figure 3. Absorption spectra of *R. capsulatus* entrapped in the PDA matrix (*R.caps*-PDA) in the absence (upper panel, upper traces) or in presence of 300 μM 2,4-DNP (upper panel, lower traces) obtained immediately after sample preparation (black lines) or after 1 h of incubation (blue lines); heat-treated cells of *R. capsulatus* entrapped in PDA and exposed to 300 μM 2,4-DNP (lower panel).

Figure 4. (A) Fluorescence spectra obtained after a 2 h incubation with FDA for (1) living *R. capsulatus* cells entrapped in the PDA matrix (*R. caps*-PDA), (2) *R.caps*-PDA exposed to 300 μM 2,4-DNP, and (3) dead cells of *R. capsulatus* entrapped in PDA obtained after heat-treatment for 2 h at 120 °C (*R.caps$_{HT}$*-PDA). Excitation at 488 nm with 2.5 nm slit, emission window from 510 to 620 nm with 5 nm slit, using a 1 cm thick cuvette. (B) Comparison of maximum fluorescence intensities at 532 nm for the different samples evaluated.

and 860 nm and the appearance of a peak at 770 nm typical of free bacteriochlorophylls (lower panel). The large difference between the intensity in the two spectra is due to most of the denaturated cellular components precipitating during the heating procedure.

Accordingly, it can be concluded that the exposure to 300 μM 2,4-DNP does not significantly affect the photosynthetic apparatus, and the loss in current obtained in the cyclic voltammetry studies cannot be related to the damaging of such system.

The quantitative evaluation of *R. capsulatus* cells viability in presence of 2,4-DNP was then performed by spectrofluorimetry by utilizing fluorescein diacetate.[38] The fluorescence spectra and the histograms presented in Figure 4 demonstrated that the long exposure to 2,4-DNP (trace 2, *R.caps*-PDA + 300.0 μM 2,4-DNP) did not result in a complete inhibition of bacteria viability, since a clear fluorescence emission signal was observed. However, a small decrease in fluorescence intensity ($23 \pm 5\%$) in relation to the fluorescence response of living *R. capsulatus* cells entrapped in PDA matrix (trace 1, *R.caps*-PDA) was obtained, indicating that a limited inhibition effect of 2,4-DNP is present. For comparison, the fluorescence response of heat-treated *R. capsulatus* cells, obtained by heat-treatment for 2 h at 120 °C, is negligible as shown in Figures 4A (trace 3) and 4B. The different fluorescence response is due to the absence of active membrane-associated and intracellular esterases in dead
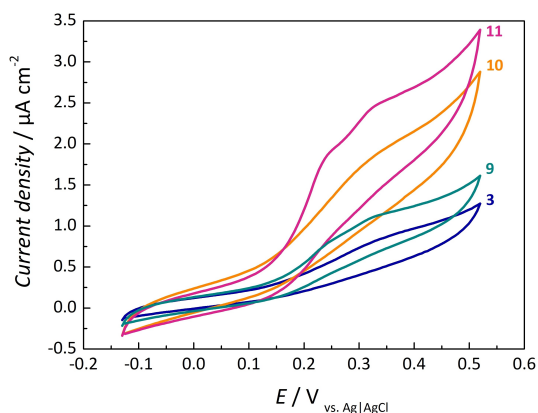
bacterial cells, which are required to accomplish the hydrolyzation of FDA to the fluorescent fluorescein.

2,4-DNP interaction with *R. capsulatus* in PDA

To further clarify the effect of 2,4-DNP on the metabolism of purple bacteria, photobioelectrocatalytic studies with 2,4-DNP were performed also in presence of ortophenantroline (*o*-phen), an inhibitor of the photosynthetic electron transfer chain (Figure 5). First, the cyclic voltammograms of the *R.caps*-PDA biohybrid photoanodes with malic acid in presence of 100 μM *o*-phen revealed an increase in current generation, passing from $1.50 \pm 0.35 \ \mu A \, cm^{-2}$ (trace 3, no *o*-phen) to $2.54 \pm 0.45 \ \mu A \, cm^{-2}$ (trace 10). As previously discussed for the cyclic voltammetries of Figure 1, also in this case only one broad redox peak is obtained at a potential of about $+0.31 \ V$, due to the extracellular electron transfer process mediated by PDA.

It is known that in the photosynthetic electron transport chain of purple bacteria *o*-phen inhibits the electron transfer from primary semiquinone (Q_A^-) to secondary oxidized quinone

ChemElectroChem

Research Article
doi.org/10.1002/celc.202300013

**Chemistry
Europe**
European Chemical
Societies Publishing

Figure 5. Cyclic voltammetries for the biohybrid photoanodes under light in presence of 50 mM malic acid + 45 mM ethanol: (3) *R.caps*-PDA, (9) *R.caps*-PDA + 100 μM 2,4-DNP, (10) *R.caps*-PDA + 100 μM *o*-phen, (11) *R.caps*-PDA + 100 μM *o*-phen + 100 μM 2,4-DNP. Scan rate, 1 mV s^{-1}; CE, Pt; RE, Ag|AgCl (3 M NaCl).

(Q_B) by competitive binding at the Q_B site (pathway 1, Scheme 1).[39,40] This leads to the rapid return of electrons from Q_A^- to the oxidized bacteriochlorophyll P870.[41] Accordingly, the inhibition of primary photochemistry and block of secondary electron transport (pathway 2, Scheme 1) are the two effects caused by *o*-phen.[37] Hence, in the presence of the PDA matrix acting as an artificial electron "sink" (pathway 5, Scheme 1); blocking the natural electron flow in the photosystem using *o*-phen results in the electrons generated in the charge separation process (P870→P870*) being more easily diverted to the electrode surface via the primary quinone acceptor of the reaction center (pathway 4, Scheme 1), in agreement with the marked increase in current density observed in presence of *o*-phen (trace 10). This is consistent with the finding of Vermeglio et al. that in presence of both *o*-phen, blocking the $Q_A^-Q_B \rightarrow Q_AQ_B^-$ electron transfer, and an electron donor reducing the oxidized P870, Q_A^- could be oxidized by a surrounding electron acceptor.[42] Furthermore, it should be noted that an increase in photocurrent response in presence of an inhibitor of the photosynthetic electron transfer chain at the Q_A–Q_B step was recently reported also by Saper et al. using 3-(3,4-dichlorophenyl)-1,1-dimethylurea (DCMU) with cyanobacteria-based photoelectrodes.[43]

Additionally, when 2,4-DNP is added together with *o*-phen (trace 11), the current density is further enhanced in comparison to both trace 9 (presence of 2,4-DNP in absence of *o*-phen) and trace 10, achieving 3.7 ± 0.5 μA cm^{-2}, indicating a photoelectrocatalytic oxidation process taking place in the photosystem of *R. capsulatus*, with 2,4-DNP acting as an electron donor. Two redox peaks are obtained in the presence of 2,4-DNP, as previously discussed for Figure 1, also in presence of *o*-phen, confirming that the presence of the contaminant allows an additional extracellular electron transfer pathway. Under these conditions the energy conversion efficiency, considering the light intensity provided (153 mW cm^{-2}), achieved the maximum value of 0.01%, up from 0.005% when no *o*-phen is added. While this is a low value, it must be considered that: (i)

the energy conversion efficiency (from photon to ATP production) of photosynthetic purple bacteria varies between 4 and 0.1% depending on light conditions,[44] and (ii) the current experimental setup is not aimed, nor optimized, to maximize the efficiency of the process.

The energy cascade in the photosynthetic unit has the role to funnel electronic excitations from the light-harvest complexes, creating a reservoir of photoexcited electrons from which the reaction center drains the excess of electrons, redirecting them into different metabolic pathways.[45] This process allows preventing the overreduction of the cyclic electron transport system in specific conditions, such as under excess of illumination or in presence of electron donors (organic substrates).[24] Therefore, during photoheterotrophic grow of *R. capsulatus*, redox homeostasis is achieved through the interplay of cyclic photosynthetic electron transport and the coordinate control of various redox-balancing mechanisms (i.e., Calvin-Benson-Bassham, CBB cycle; Dimethylsulfoxide reductase, DMSOR system; or dinitrogenase system) occurring in the ubiquinone pool. Each system can employ a different terminal electron acceptor and the hierarchy of redox pathways was shown to be under cellular control wherein the normal regulatory constraints are overcome to insure redox balance.[46,47] Thus, variations in the concentration of substrates that are relevant for the regulatory mechanism promote a change in the electron pathway. Given the above considerations and the obtained electrochemical and spectroscopic evidence, it can be concluded that the long-term exposure of *R. capsulatus* to concentrations as high as 300 μM 2,4-DNP did not cause the damage to the antenna apparatus nor a significant inhibition or complete death of the cells. Therefore, the decrease in current response of the *R.caps*-PDA biohybrid electrodes under illumination in presence of high concentrations of 2,4-DNP (from 100 to 300 μM) is attributed to the electrons being re-directed toward an alternative electron sink. Blasco and Castillo reported that *R. capsulatus* has a 2,4-DNP photoreduction pathway performed by enzymes with nitrophenol reductase-activity (NPR) requiring NAD(P)H as an electron donor.[33,34] NPR, located in the cytosol, was identified as an inducible reductase that could function as a detoxifying enzyme, exhibiting activity also toward other polynitrophenols such as 2,5-DNP, 3,4-DNP and 2,4,6-TNP.[48] Interestingly, the photoreduction of 2,4-DNP has been reported also for other photosynthetic bacteria such as *Anabaena variabilis*.[49] For *R. capsulatus*, 2,4-DNP was found to serve neither as carbon nor as nitrogen source, making its photoanaerobic metabolization a cometabolic reductive process requiring alternative sources of carbon and nitrogen, and being regulated by the intracellular C/N ratio.[33,34,50] Scheme 1 shows the proposed photoreduction of 2,4-DNP in NPR enzyme as the alternative electron sink diverting electrons from the extracellular electron transfer, and the effect of *o*-phen on the photosynthetic apparatus of *R. capsulatus*. In should be underlined that Scheme 1 reports a simplified, not comprehensive, metabolic pathway for 2,4-DNP reduction, since multiple products could be obtained from 2,4 DNP assimilation in purple bacteria. Accordingly, future studies should be performed to elucidate the complete metabolic

process of 2,4-DNP in purple bacteria biophotoelectrodes. The analysis of the 2,4-DNP reduction products and real-time determination of NADPH production would be of great interest. At this purpose, the approach recently reported by Shlosberg et al. to characterize NADPH secretion from cyanobacteria cells under electrochemical polarization and illumination could be employed in future studies to elucidate this process.[51]

Conclusion

The development of sustainable approaches for the early, distributed, and in-situ monitoring of critical water pollutants is of the utmost importance to avoid and/or minimize the release of toxic compounds in the environment. Herein, we have demonstrated that the current generation of a sustainable intact PNSB-based photoelectrode operating in neutral conditions is clearly affected by the presence of 2,4-DNP in a range of concentrations relevant to the limits of acute and chronic toxicity. The system does not require rare metal catalysts, critical raw materials, nor the time-consuming synthesis of redox polymers, making it of particular interest for the development of self-powered biosensors performing in-situ monitoring. Furthermore, the viability of the bacterial cells and the activity of their photosynthetic apparatus were not significantly affected, even at concentrations as high as 300 µM, allowing the operation of the biosensor at high concentration of the contaminant. Future studies should focus on the possibility that PNSB divert electrons toward a reductive metabolism of 2,4-DNP, which would make the technology relevant to accomplish both the sun-powered in-situ monitoring of the contaminant and its simultaneous removal. Finally, maximizing the stability of the photobioelectrocatalytic system developed will also be critical in view of its possible application for environmental remediation purposes.

Experimental Section

Chemicals

All chemicals were used as received without further purification. Ultrapure Milli-Q water (18 MΩ cm^{-1}) was used for the preparation of all the solutions.

Bacterial growth

Rhodobacter capsulatus strain DSM 152 was obtained from the German Collection of Microorganisms and Cell Cultures (DSMZ) and grown at 10% *v/v* in sterile 50 mL bottles sealed with airtight stoppers, containing liquid growth medium comprised of malic acid (4.0 g L^{-1}), (NH$_4$)$_2$SO$_4$ (1.0 g L^{-1}), CaCl$_2$·2H$_2$O (75 mg L^{-1}), MgSO$_4$·7H$_2$O (200 mg L^{-1}), FeSO$_4$·7H$_2$O (12 mg L^{-1}), EDTA (20 mg L^{-1}), thiamine (1 mg L^{-1}), biotin (15 mg L^{-1}), K$_2$HPO$_4$ (0.9 g L^{-1}), KH$_2$PO$_4$ (0.6 g L^{-1}) and a trace elements solution (1 mL L^{-1}) previously prepared.[11] The pH of the medium was adjusted to 6.8 using 5 M NaOH, and the growth medium was sterilized (Systec VX-55) at 125 °C for 25 min. Trace elements, MgSO$_4$, CaCl$_2$, FeSO$_4$, and biotin were added to the medium after

sterilization by filtration through a 0.20 µm filter (Puradisc 25). The growth procedure was performed at 28 °C in an incubator (IKA KS 3000 i control) under illumination provided by an incandescent lamp (80 W).

Preparation of biohybrid photoanodes

The preparation of biohybrid electrodes was performed following the procedure previously described.[18] Briefly, *R. capsulatus* cells were collected after 72 h growth following a two-step centrifugation procedure; the first step was carried out at 4000 *g* for 20 min at 20 °C (MPW-260R Centrifuge) and the second, at 12000 rpm for 15 min (Eppendorf Centrifuge 5424R). After obtaining the pellets of *R. capsulatus*, the electrodes were ready to use in less than 90 minutes, starting with the aerobic polymerization of PDA (5 mM dopamine hydrochloride in MOPS buffer at pH 8.0) in presence of bacterial cells (1 g mL^{-1}) during 60 min under magnetic stirring at 500 rpm (Metrohm 728 Magnetic Stirrer). The obtained suspension was then deposited on a glassy carbon electrode (1 uL mm^{-1} diameter) and, after drying, it was subjected to electrochemical polymerization (PalmSens4 potentiostat) by cyclic voltammetry at 20 mV s^{-1} in MOPS buffer at pH 7. This allowed creating the biohybrid photoanodes (*R.caps*-PDA) with the formation of a redox-adhesive polydopamine matrix surrounding the bacterial cells.

Electrochemical measurements

The effects of 2,4-DNP on the photobioelectrocatalytic activity of *R. capsulatus* was evaluated by cyclic voltammetries (PalmSens4 potentiostat) performed in triplicate in a single chamber three-electrode electrochemical cell containing 35 mL of electrolyte (10 mM MgCl$_2$ and 50 mM malic acid in 20 mM MOPS buffer, pH 7). Two cycles were always performed, in the range of −0.13 V to 0.52 V at 1 mV s^{-1}, and the second cycle is always utilized for the comparison of the (bio)electrodes. A Pt wire was used as the counter electrode, an Ag|AgCl (3 M NaCl, Basi MF2052) electrode was the reference electrode, and the *R.caps*-PDA photoanode was the working electrode. Control experiments were performed with bare glassy carbon electrodes as well as with glassy carbon electrodes coated with only PDA (sterile electrodes), in the absence of *R. capsulatus* cells, and with heat-treated *R. capsulatus* cells for 2 h at 120 °C (*R.caps$_{HT}$*-PDA). Prior to the photoelectrochemical studies, the electrolyte was saturated with Argon (99.99%) for 10 min, keeping the same flow on top of the electrochemical cell during the experiments. A fiber optic lamp (Schott KL 1500 LCD) equipped with a light bulb of 10 W was utilized to illuminate the electrodes, providing a light intensity of 153 mW cm^{-2} (measured with Gigahertz-Optik MSC15). The *R.caps*-PDA electrodes were exposed to different concentrations of 2,4-DNP, in a range from 0.5 to 300 µM. The stock solutions of 2,4-DNP were prepared by solubilization of the contaminant in 20% ethanol + 20% of dimethyl sulfoxide (DMSO), with the purpose of maintaining the final concentration of ethanol in the electrochemical cell at 45 mM. Thus, the electrochemical experiments with 2,4-DNP were performed with the electrolyte containing both malic acid and ethanol, the first as carbon source and the second used for the solubilization of dinitrophenol. For the comparison of the photobioelectrocatalytic activities of the *R.caps*-PDA electrodes, the current densities were evaluated based on the anodic photocurrent obtained for the second cycle of each voltammetric curve at +0.40 V, with the average values presented together with the respective standard deviation. For a deeper evaluation of the effect of 2,4-DNP on photobioelectrocatalysis of *R. capsulatus*, we used the photosystem inhibitor orthophenantroline (*o*-phen). For these studies, the *R.caps*-PDA electrodes were exposed to 100 µM *o*-phen in the absence

ChemElectroChem

Research Article
doi.org/10.1002/celc.202300013

Chemistry Europe
European Chemical
Societies Publishing

and presence of 100 μM 2,4-DNP. The *o*-phen stock solution was also prepared in 20% ethanol + 20% DMSO, to keep constant the concentration of ethanol in the electrolyte.

Spectrophotometric and Spectroscopic fluorescence studies

The viability of *R. capsulatus* cells after being exposed to 2,4-DNP was determined by spectrofluorimetric measurements with the samples (1) living cells of *R. capsulatus* entrapped in the PDA matrix (*R.caps*-PDA), (2) *R.caps*-PDA exposed to 300 μM 2,4-DNP, and (3) dead cells of *R. capsulatus* entrapped in PDA obtained after heat-treatment for 2 h at 120°C *R.caps*$_{HT}$-PDA. The samples were prepared as follows: *R. capsulatus* cells were collected according to the centrifugation procedures previously described, proceeding with the aerobic polymerization for 1 h. After this step, the matrix was collected by centrifugation at 12000 rpm for 15 min and further resuspended in MOPS buffer at pH 7.0. The obtained suspension was splitted to obtain the samples for quintuplicates measurements. For sample (2), aliquots of 8 mM 2,4-DNP stock solution were added to obtain the final concentration of 300 μM in the replicates. All samples were incubated overnight at room temperature. Following, 6 μL of fluorescein diacetate (FDA) (1 mg mL^{-1} in acetone) was added to 2 mL of sample, containing 1.9 mL MOPS buffer at pH 7.0 and 100 μL of suspensions, and further incubated for 2 h. Signals of fluorescent molecules were detected using a Varian Cary Eclipse Fluorescence Spectrophotometer, with excitation at 488 nm and emission window from 495 to 650 nm. The excitation and emission slit were 2.5 and 5 nm, respectively. Hence, based on the fluorescence intensity observed after this period of incubation, the viability of cells exposed to 2,4-DNP (2) was compared with those not exposed to 2,4-DNP (1) as well as with the response obtained with heat-treated bacteria (3). To evaluate possible damages to the photosynthetic apparatus of *R. capsulatus* after exposure to 2,4-DNP, the absorption spectra of the samples (1) and (2) were recorded immediately after sample preparation and after 1 h of incubation in presence of dinitrophenol, in the range 400–1000 nm using a Cary 5000 UV-Vis-NIR spectrophotometer (Agilent Technologies). The spectra of sample (3) and 2,4-DNP were also obtained for comparison.

Conflict of Interest

The authors declare no conflict of interest.

Data Availability Statement

The data that support the findings of this study are available from the corresponding author upon reasonable request.

[1] G. Drews, J. F. Imhoff, in *Variations in Autotrophic Life*, **1991**, pp. 51–97.
[2] J. F. Imhoff, in *Anoxygenic Photosynthetic Bacteria* (Eds.: R. E. Blankenship, M. T. Madigan, C. E. Bauer), Springer Netherlands, Dordrecht, **1995**, pp. 1–15.
[3] X. Hu, T. Ritz, A. Damjanović, F. Autenrieth, K. Schulten, *Q. Rev. Biophys.* **2002**, *35*, 1–62.
[4] G. Feher, J. P. Allen, M. Y. Okamura, D. C. Rees, *Nature* **1989**, *339*, 111–116.
[5] J. P. Allen, J. C. Williams, *FEBS Lett.* **1998**, *438*, 5–9.
[6] A. Operamolla, R. Ragni, F. Milano, R. Roberto Tangorra, A. Antonucci, A. Agostiano, M. Trotta, G. Farinola, *J. Mater. Chem. C* **2015**, *3*, 6471–6478.
[7] L. D. de M. Torquato, M. Grattieri, *Curr. Opin. Electrochem.* **2022**, *34*, 101018.
[8] A. Kumar, L. H.-H. Hsu, P. Kavanagh, F. Barrière, P. N. L. Lens, L. Lapinsonnière, J. H. Lienhard, V. U. Schröder, X. Jiang, D. Leech, *Nat. Chem. Rev.* **2017**, *1*, 0024.
[9] G. Pankratova, L. Gorton, *Curr. Opin. Electrochem.* **2017**, *5*, 193–202.
[10] N. S. Weliwatte, M. Grattieri, S. D. Minteer, *Photochem. Photobiol. Sci.* **2021**, *20*, 1333–1356.
[11] M. Grattieri, Z. Rhodes, D. P. Hickey, K. Beaver, S. D. Minteer, *ACS Catal.* **2019**, *9*, 867–873.
[12] G. Longatte, A. Sayegh, J. Delacotte, F. Rappaport, F.-A. Wollman, M. Guille-Collignon, F. Lemaître, *Chem. Sci.* **2018**, *9*, 8271–8281.
[13] A. Sayegh, L. A. Perego, M. Arderiu Romero, L. Escudero, J. Delacotte, M. Guille-Collignon, L. Grimaud, B. Bailleul, F. Lemaître, *ChemElectroChem* **2021**, *8*, 2968–2978.
[14] F. Dong, Y. S. Lee, E. M. Gaffney, W. Liou, S. D. Minteer, *ACS Catal.* **2021**, *11*, 13169–13179.
[15] A. Antonucci, M. Reggente, C. Roullier, A. J. Gillen, N. Schuergers, V. Zubkovs, B. P. Lambert, M. Mouhib, E. Carata, L. Dini, A. A. Boghossian, *Nat. Nanotechnol.* **2022**, *17*, 1111–1119, DOI 10.1038/s41565-022-01198-x.
[16] K. Hasan, S. A. Patil, K. Górecki, D. Leech, C. Hägerhäll, L. Gorton, *Bioelectrochemistry* **2013**, *93*, 30–36.
[17] M. Grattieri, S. Patterson, J. Copeland, K. Klunder, S. D. Minteer, *ChemSusChem* **2020**, *13*, 230–237.
[18] G. Buscemi, D. Vona, P. Stufano, R. Labarile, P. Cosma, A. Agostiano, M. Trotta, G. M. Farinola, M. Grattieri, *ACS Appl. Mater. Interfaces* **2022**, *14*, 26631–26641.
[19] M. Ambrico, P. Ambrico, A. Minafra, A. De Stradis, D. Vona, S. Cicco, F. Palumbo, P. Favia, T. Ligonzo, *Sensors* **2016**, *16*, 1946.
[20] O. Simoska, E. M. Gaffney, S. D. Minteer, A. Franzetti, P. Cristiani, M. Grattieri, C. Santoro, *Curr. Opin. Electrochem.* **2021**, *30*, 100762.
[21] M. Grattieri, S. D. Minteer, *ACS Sens.* **2018**, *3*, 44–53.
[22] M. Grattieri, H. Chen, S. D. Minteer, *Chem. Commun.* **2020**, *56*, 13161–13164.
[23] M. Masi, P. Bollella, M. Riedel, F. Lisdat, E. Katz, *ACS Appl. Energ. Mater.* **2020**, *3*, 9543–9549.
[24] M. Grattieri, *Photochem. Photobiol. Sci.* **2020**, *19*, 424–435.
[25] M. Rani, Rachna, J. Yadav, U. Shanker, *Environ. Nanotechnol. Monit. Manag.* **2020**, *14*, 100325.
[26] United States Environmental Protection Agency (EPA), *Water-Related Environmental Fate of 129 Priority Pollutants*, **1979**.
[27] J. I. Kwak, S. W. Kim, L. Kim, R. Cui, J. Lee, D. Kim, Y. Chae, Y.-J. An, *Aquat. Toxicol.* **2020**, *228*, 105646.
[28] L. Politi, C. Vignali, A. Polettini, *J. Anal. Toxicol.* **2007**, *31*, 55–61.
[29] R. Xie, N. Zhang, Y. Qu, M. Tang, F. Zhang, F. Chai, Z. Su, *Nanotechnology* **2021**, *33*, 025501.
[30] H. Dejmkova, A.-I. Stoica, J. Barek, J. Zima, *Talanta* **2011**, *85*, 2594–2598.
[31] A. Godain, M. W. A. Spurr, H. C. Boghani, G. C. Premier, E. H. Yu, I. M. Head, *Front. Environ. Sci.* **2020**, *8*, 5.
[32] Y. Liu, K. Ai, L. Lu, *Chem. Rev.* **2014**, *114*, 5057–5115.
[33] R. Blasco, F. Castillo, *Appl. Environ. Microbiol.* **1992**, *58*, 690–695.
[34] R. Blasco, F. Castillo, *Pestic. Biochem. Physiol.* **1997**, *58*, 1–6.
[35] R. A. Brunisholz, H. Zuber, *J. Photochem. Photobiol. B* **1992**, *15*, 113–140.
[36] P. Qian, D. J. K. Swainsbury, T. I. Croll, J. H. Salisbury, E. C. Martin, P. J. Jackson, A. Hitchcock, P. Castro-Hartmann, K. Sader, C. N. Hunter, *Biochem. J.* **2021**, *478*, 3775–3790.
[37] R. K. Clayton, H. Fleming, E. Z. Szuts, *Biophys. J.* **1972**, *12*, 46–63.

[38] G. Bedendi, L. D. De Moura Torquato, S. Webb, C. Cadoux, A. Kulkarni, S. Sahin, P. Maroni, R. D. Milton, M. Grattieri, *ACS Meas. Sci. Au* **2022**, *2*, 517–541.

[39] M. Y. Okamura, R. A. Isaacson, G. Feher, *Proc. Natl. Acad. Sci. USA* **1975**, *72*, 3491–3495.

[40] N. Ginet, J. Lavergne, *Biochemistry* **2001**, *40*, 1812–1823.

[41] F. Mavelli, M. Trotta, F. Ciriaco, A. Agostiano, L. Giotta, F. Italiano, F. Milano, *Eur. Biophys. J.* **2014**, *43*, 301–315.

[42] A. Vermeglio, T. Martinet, R. K. Clayton, *Proc. Natl. Acad. Sci. USA* **1980**, *77*, 1809–1813.

[43] G. Saper, D. Kallmann, F. Conzuelo, F. Zhao, T. N. Tóth, V. Liveanu, S. Meir, J. Szymanski, A. Aharoni, W. Schuhmann, A. Rothschild, G. Schuster, N. Adir, *Nat. Commun.* **2018**, *9*, 2168.

[44] M. Sener, J. Strumpfer, A. Singharoy, C. N. Hunter, K. Schulten, *eLife* **2016**, *5*, e09541.

[45] X. Hu, A. Damjanović, T. Ritz, K. Schulten, *Proc. Natl. Acad. Sci. USA* **1998**, *95*, 5935.

[46] M. A. Tichi, F. R. Tabita, *J. Bacteriol.* **2001**, *183*, 6344–6354.

[47] M. A. Tichi, F. R. Tabita, *Arch. Microbiol.* **2000**, *174*, 322–333.

[48] R. Blasco, F. Castillo, *Appl. Environ. Microbiol.* **1993**, *59*, 1774–1778.

[49] T. Hirooka, H. Nagase, K. Hirata, K. Miyamoto, *Biochem. Eng. J.* **2006**, *29*, 157–162.

[50] M. Alexander, *Science* **1981**, *211*, 132–138.

[51] Y. Shlosberg, B. Eichenbaum, T. N. Tóth, G. Levin, V. Liveanu, G. Schuster, N. Adir, *iScience* **2021**, *24*, 101892.

RESEARCH ARTICLE

Purple bacteria photobioelectrocatalysis: 2,4-Dinitrophenol affects the photobioelectrocatalysis of biohybrid photoelectrodes based on intact photosynthetic bacteria paving the way for the development of biosensors for the early monitoring of this contaminant.
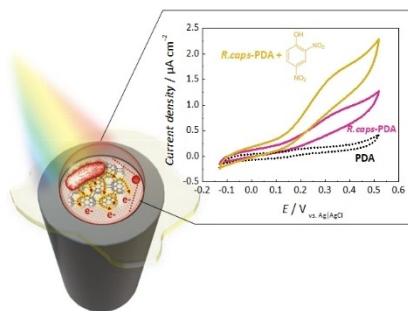
Dr. L. D. de Moura Torquato, R. M. Matteucci, Dr. P. Stufano, Dr. D. Vona, Prof. G. M. Farinola, Dr. M. Trotta, Prof. M. V. Boldrin Zanoni, Dr. M. Grattieri*

1 – 10

Photobioelectrocatalysis of Intact Photosynthetic Bacteria Exposed to Dinitrophenol